DER Simulation of the World Highest Jumping Robot

Junlin Chen[1] and Sanskar Nalkande[2]

I. INTRODUCTION AND BACKGROUND

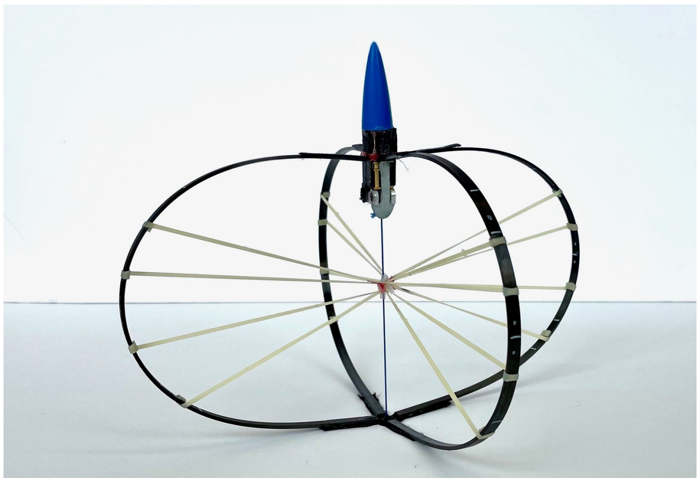

Fig. 1. The presented jumper with the hybrid spring in a stable pre-jump configuration [2]

This little robot can jump higher than anything in the world and weighs less than a tennis ball. This jumper can soar 31 meters above the ground, over a ten-story structure. It may leap to eye level from the feet of the Statue of Liberty. For something to count as a jump, it must satisfy two criteria. First, motion must be created by pushing off the ground, and second, no mass can be lost, so, rockets constantly ejecting burnt fuel are not jumping.

A. How does it work?

Four carbon fiber sections connected by elastic bands make up the basic structure. Together, they form a spring that holds all the energy required for the jump. A tiny motor is located at the top of the robot, and a string that is fastened to the bottom is coiled around the axle. Thus, the robot is compressed by the string when the motor is turned on, storing energy in the rubber bands and carbon fiber.

The latch keeping the string on the axle is now released by means of a trigger. Thus, the spring releases its stored energy when the entire string unspools at once. It takes the jumper nine milliseconds to travel from a complete stop to over 100 km/h. This results in an acceleration of more than 300 g. This jumping process can be seen in the image below.

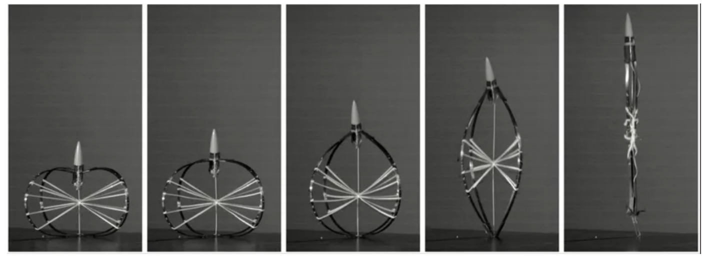

Fig. 2. Frames from Launch Video in the acceleration phase [2]

B. Different Models

While we are dealing with a four armed robot, there are other robots which are modelled, tested and simulated earlier. Some of them have different geometries but the underlying concept of storing the energy gradually and releasing it in a burst remains the same. Below, are some of the alternate structures:

1) One-legged robot: The one legged jumping robot simply consists of two arms joined by a hinged motor and a weight attached on top of it. The hinged motor gradually unwinds and decreases the angle between the two arms of the robot. Now the motor quickly applies the torque and the robot jumps in the air. All of this is explained in detail in a paper by D. Tian et al.[4] But since only rigid body motion is involved in this process, it is not of any particular interest to us since we are trying to simulate a flexible and soft robot.

2) Three-legged robot: This three legged structure is majorly similar to the four legged one in regards to the energy that is stored in the rubber bands tied on the arms. But the difference arises in the flexibility of the three legs. In our case, the robot also stores energy in its bent legs. Here's an image of the three legged robot in it's jumping process:

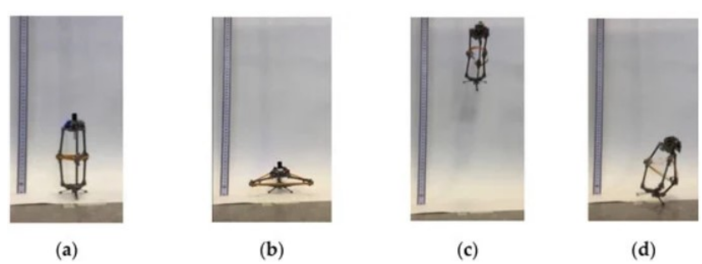

Fig. 3. The three legged jumper [3]

Although this robot is different from our one, it is of significant importance for us since the energies of the three elastic bands have been already been derived in the paper by Y.

Yan et al.[3] This would help us in deriving the energy stored in the four legged robot. The same paper also discusses the maximum jumping height of the robot. The maximum jumping height is the quantifiable metric in our simulation. We might be able to compare the effects of discretization and compare it with the theoretical results.

II. SIMULATION

Now, we talk about the process of replicating the motion of this robot in a simulation. For the simulation, we need to start by defining the geometry, material properties and the boundary conditions of the robot.

A. Geometry

The structure of the robot can be replicated in the simulation using geometric calculations and setting the DOF vector for the nodes accordingly. The structure in its natural and stretched form should look like this:

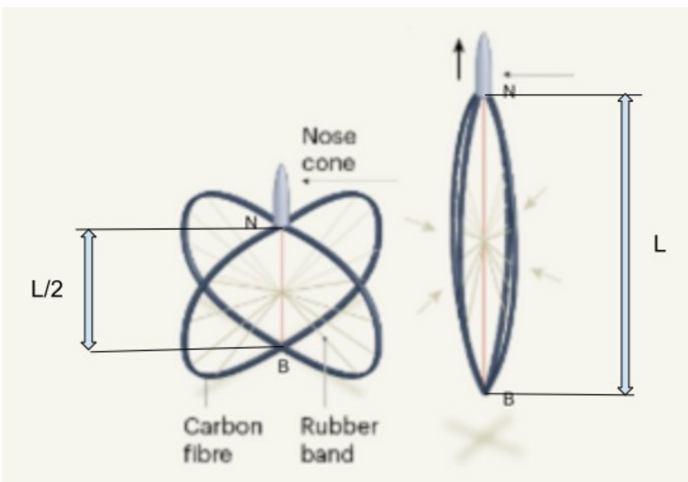

Fig. 4. Geometry of the Jumper in pre and post jump configurations [1]

There are two types of flexible structures in this robot, the carbon fiber bow and the elastic rubber bands. We can use the real life properties of these materials And then we can set the boundary conditions such that it starts in the energised form.

B. Boundary Conditions

For implementing the boundary conditions, we can introduced a third type of material, the string that connects the nose cone 'N' and the bottom junction 'B'. By setting the elastic modulus of this string very high compared to the other materials, we can make this rope virtually non-stretchable.

Suppose t_{trig} is the time at which we want to trigger the launch. Hence we set the natural length of the rope before this time to be half of the natural length in the relaxed configuration. And immediately after the jump is triggered, we make the rope to return to its original length.

The above boundary condition may be implemented using a simple conditional:

$$l_{rope} = \begin{cases} \frac{l_{natural}}{2}, & \text{if } t \leq t_{trig} \\ l_{natural}, & \text{otherwise} \end{cases}$$

C. Environment

There are three major environmental factors which affect the motion of our robot:

1) Contact with Ground: The robot gets accelerated mainly due to the contact force from the ground. Hence implementing a rigid contact is necessary.

2) Gravity: Gravity is the main force that slows down our robot and affects the maximum height it can reach. It is a constant force acting upon the robot at all times

3) Air resistance: When the robot is in motion, its motion is also dampened due to the air resistance. It can be represented simply by a force proportional to the velocity acting in its opposite direction.

III. MODELING DECISION

Given the focus of this project is the jumping robot designed by the UCSB, the simulation model will be the DER version of the real world model. However, to construct such DER solver, a few decisions has to be made on the physical properties of the robot to convert the structure into points and edges.

A. Material Decisions

According to the UCSB research[2], the hyper-tension-compression bow is the main source of energy. The material of the elastic bow includes of carbon fiber reinforced bow, ballistic nylon hinge, and rubber bands. Among them, carbon fiber bow and rubber bands are the primary elastic energy source for the robot.

No specific data is provided regarding the model name of the carbon fiber, neither its fiber orientation. Still, given the purpose of choosing carbon fiber material is for the high E/rho ratio[2], as stated in the nature paper, carbon fiber LY5/5 from Rahmani's research[5] is chosen for its highest Young's modulus.

The rubber bands used on the robot are also unknown except that they are made of latex and the total mass is 12.4g. An experimental review of rubber bands reveals that rubber bands are highly unlinear during stretching cycling and has high residual strain when unstressed[6]. Hence, even though DER is known for simulating non-linear behavior, DER may not be able to simulate the performance of the robot after a few cycles. To narrow the focus of this project, the simulation will only run once to avoid any inaccuracy from repeated cycling.

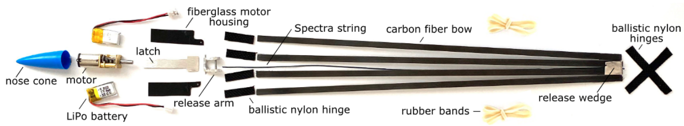

Fig. 5. Material Layout of the Jumping Robot from Hawkes et al.[2]

B. Structural Decisions

The novel idea about the UCSB structural design is that it use "engineered" jumper rather than biological drive system. Through the use of gears, elastic energy of the system can be "stored" stability by the continuous running of motor and therefore allows more work to be done per jump. Given this feature, the electric motor power will no longer be a main constraint of producing elastic energy as it is in biological drive system.

To put this in the context of simulation, there will be a constant external force applied at the joint of the bows until the mechanism is released. Again, the specification of the electric motor used in the research is not provided. Hence we will be going with the simplified boundary conditions explained in the simulation section.

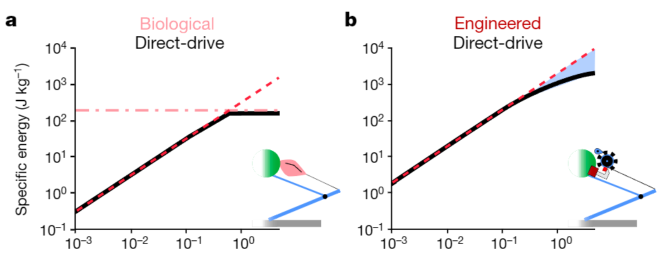

Fig. 6. Biological Direct Drive vs. Engineered Direct Drive from Hawkes et al.[2]

In addition, their research had built upon the previous researches and created the new hybrid tension-compression mechanism, which basically combined compression-bow and a spring linkage. They claims their selection of model provides higher specific energy than tension linkage or compression bow alone[2]. Thus, the simulation will be using this hybrid simulation as the geometry model. This means there will be both carbon fiber bows and latex rubber bands in the simulated system.

The full composition of the jumping robot includes a hybrid tension-compression cage, an electric motor, four nylon hinges and an actuation mechanism. However, for simplicity and best utilization of class knowledge, this project will only be simulating the tension-compression part of the robot, which has four carbon fiber bows as the main structure and a handful of rubber bands assisting the bows.

According to Hawkes et al.[2], rubber bands are necessary to reduce the max strain of the carbon fiber and to form the tension linkage. In real life, mechanism preventing the failure of carbon fiber is necessary to ensure the reliability of the robot given the unpredictability of composite materials. In simulation, the carbon fiber bows will not fail under DER assumptions, meaning the implementation of rubber bands only serve the purpose of improving system performance.

In terms of bows, the carbon fiber bows are in minimal energy state when they are straight(natural K = 0). Elastic energy are stored by increasing the curvature of the rods as electric motor exerts force and bending them. The maximum amount of deformation in simulation is chosen to reflect the real world demo of the jumping robot after 32 seconds.(just before the actuation)

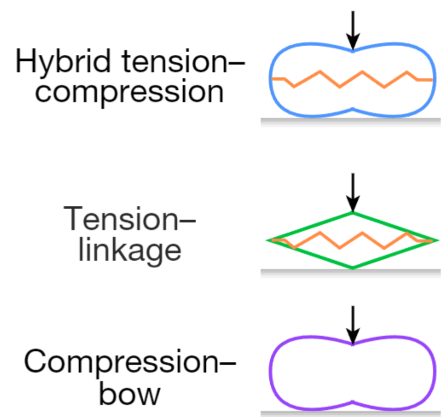

Fig. 7. Different Elastic Structure Design Layout from Hawkes et al.[2]

IV. IMPORTANCE OF THE PROJECT

There are various reasons why a robot need jumping capability. For two-legged robots or track based/wheel based robots, their ability to cross rough terrains are limited by their physical parameters (i.e. track length, leg height) and ground surface properties(sandy, muddy, etc).

On the other hand, a jumping robot of any size may overcome the roughest terrain by simply "flying" over it. On low gravity environments, such as the moon, the UCSB robot will be able to leap 180 meters in height given the gravity is only one sixth of the Earth gravity. A jump at this height, if can be directed precisely, have the potential to be utilized as a means of movement to overcome craters and canyon on extraterrestrial surfaces.

Furthermore, given the main driving components are just carbon fiber bows and electric motor, jumping robots can be made lighter than traditional robots with legs or track. As the result, there is clearly a perspective market for this type of robots for extraterrestrial exploration to go across terrains that are unimaginable to go across for existing robots and rovers.

The simulation method that is going to be implemented in the project will serve as a basis for designing such robots. By conducting parametric studies before building physical prototypes, the design cost and design time can be greatly reduced.

Fig. 8. Example Photo of Rough Moon Surface from NASA[6]

V. TIMELINE AND CHALLENGES

TABLE I
TIMELINE TABLE

Date	Challenge to be done
Nov.5	Presentation and proposal write up
Nov.13	Simulation for a single bow ready
Nov.19	Two bow system simulated, mid-term presentation ready
Nov.27	Rubber band implementation and actuation
Dec.4	Visualization and final presentation ready
Dec.7	Final report due

REFERENCES

[1] S. Bergbreiter, "Jumping robot bests biology by enhancing stored energy," Nature, vol. 604, no. 7907, pp. 627–628, Apr. 2022, doi: 10.1038/d41586-022-01077-4.

[2] E. W. Hawkes et al., "Engineered Jumpers Overcome Biological Limits via Work Multiplication," Nature News, Apr. 27, 2022.

[3] Y. Yan, K. Smith, A. Macario-Rojas, and H. Zhang, "Simulation of the Landing Buffer of a Three-Legged Jumping Robot," Machines, vol. 10, no. 299, 2022.

[4] D. Tian, J. Gao, C. Liu, and X. Shi, "Simulation of Upward Jump Control for One-Legged Robot Based on QP Optimization," Sensors, vol. 21, no. 5, p. 1893, Mar. 8, 2021.

[5] H. Rahmani, S. H. M. Najaf, A. Ashori, and M. Golriz, "Title of the Article," Polymers and Polymer Composites, vol. 23, no. 7, pp. 475-482, 2015.

[6] NASA, "The Moon's Surface," Earth's Moon, Oct 3, 2017. https://moon.nasa.gov/resources/48/the-moons-surface/